

Probabilistic passive earth pressure analysis by the Random Finite Element Method

D. V. Griffiths, Professor
Division of Engineering, Colorado School of Mines, U.S.A.

Gordon A. Fenton, Professor
Department of Engineering Mathematics, Dalhousie University, Canada

Derena E. Tveten
Montana DOT, U.S.A.

Keywords: probabilistic, earth pressure, statistical analysis

ABSTRACT: The paper initially reviews some established probabilistic analysis techniques, such as the First Order Second Moment (FOSM), and the First Order Reliability Method (FORM), and then goes on to describe a more rigorous approach called the Random Finite Element Method (RFEM) in which random field and finite element methodologies are merged. The results highlight cases in which proper modeling of spatial correlation is important, and illustrate this through a simple example of passive earth pressure.

1. Introduction

Many sources of uncertainty exist in geotechnical analysis ranging from the material parameters to the sampling and testing techniques. This paper addresses the question of how variable material parameters impact the safety and, ultimately, the economics of geotechnical design.

Traditional geotechnical analysis uses the “Factor of Safety” approach in one of two ways. In foundations analysis for example, Terzaghi’s bearing capacity equation leads to an estimate of the ultimate value, which is then divided by the Factor of Safety to give allowable loading levels for design. Alternatively, in slope stability analysis, the Factor of Safety is included by reducing the shear strength of the soil prior to performing a limit equilibrium calculation. Either way, the Factor of Safety represents a blanket factor that implicitly includes all sources of variability and uncertainty inherent in the geotechnical analysis.

The approaches described in this paper attempt to include the effects of soil property variability in a more scientific way using statistical methods. If it is assumed that the soil parameters in question (e.g. friction angle, cohesion, compressibility and permeability) are

random variables that can be expressed in the form of a probability density function, then the issue becomes one of estimating the probability density function of some outcome that depends on the input random variables. The output can then be interpreted in terms of probabilities, leading to statements such as: “The design load on the foundation will give a probability of bearing capacity failure of $p_1\%$ ”, “The embankment has a probability of slope failure of $p_2\%$ ”, “The probability of the design settlement levels being exceeded is $p_3\%$ ”, or “The probability of the seepage level exceeding the design limit is $p_4\%$ ”.

A thorough understanding of how random variables affect the functions that depend on them is essential. The first part of the paper therefore summarizes some of the fundamental rules that describe this relationship.

2. Some rules describing random variables

In this section, the notation is quite generic with random variables (e.g. X and Y) denoted in upper case. Later in the paper, specific geotechnical examples will be included.

2.1 Expectation

Let a random variable X be described by the Probability Density Function (PDF), $f_X(x)$. If $g(X)$ is a function of the random variable X , then the expected value of $g(X)$, is its average value after it has been weighted by the Probability Density Function:

$$E[g(X)] = \int_{-\infty}^{\infty} g(x)f_X(x) dx \quad (1)$$

2.2 Moments

First Moment: Mean

$$\mu_x = E[X] = \int_{-\infty}^{\infty} xf_X(x) dx \quad (2)$$

Second Moment: Variance

$$\text{Var}[X] = \sigma_x^2 = E[(X - \mu_x)^2] = \int_{-\infty}^{\infty} (x - \mu_x)^2 f_X(x) dx \quad (3)$$

Third Moment: Skewness

$$\nu_x = \frac{E[(X - \mu_x)^3]}{\sigma_x^3} = \frac{1}{\sigma_x^3} \int_{-\infty}^{\infty} (x - \mu_x)^3 f_X(x) dx \quad (4)$$

2.3 Identities relating to Expectation

A linear function of two random variables X and Y

$$E[a + bX + cY] = a + bE[X] + cE[Y] \quad (5)$$

The sum of multiple random variables X_1, X_2, \dots etc.

$$E[X_1 + X_2 + \dots + X_n] = E[X_1] + E[X_2] + \dots + E[X_n] \quad (6)$$

The sum of functions of two random variables, X and Y

$$E[f(X) + g(Y)] = E[f(X)] + E[g(Y)] \quad (7)$$

A nonlinear function of two random variables X and Y can be expressed using a Taylor series expansion

$$\begin{aligned}
 f(X, Y) &= f(\mathbb{E}[X], \mathbb{E}[Y]) + (X - \mathbb{E}[X]) \frac{\partial f}{\partial x} + (Y - \mathbb{E}[Y]) \frac{\partial f}{\partial y} \\
 &\quad + \frac{1}{2}(X - \mathbb{E}[X])^2 \frac{\partial^2 f}{\partial x^2} + \frac{1}{2}(Y - \mathbb{E}[Y])^2 \frac{\partial^2 f}{\partial y^2} \\
 &\quad + \frac{1}{2}(X - \mathbb{E}[X])(Y - \mathbb{E}[Y]) \frac{\partial^2 f}{\partial x \partial y} \\
 &\quad + \frac{1}{2}(Y - \mathbb{E}[Y])(X - \mathbb{E}[X]) \frac{\partial^2 f}{\partial y \partial x} + \dots
 \end{aligned} \tag{8}$$

where all derivatives are evaluated at the mean. Thus to a first order of accuracy:

$$\mathbb{E}[f(X, Y)] = f(\mathbb{E}[X], \mathbb{E}[Y]) \tag{9}$$

and to a second order:

$$\begin{aligned}
 \mathbb{E}[f(X, Y)] &= f(\mathbb{E}[X], \mathbb{E}[Y]) + \frac{1}{2} \text{Var}[X] \frac{\partial^2 f}{\partial x^2} + \frac{1}{2} \text{Var}[Y] \frac{\partial^2 f}{\partial y^2} \\
 &\quad + \text{cov}[X, Y] \frac{\partial^2 f}{\partial x \partial y}
 \end{aligned} \tag{10}$$

2.4 Identities relating to Variance

Variance of a random variable X

$$\begin{aligned}
 \text{Var}[X] &= \mathbb{E}[(X - \mu_x)^2] \\
 &= \mathbb{E}[X^2] - (\mathbb{E}[X])^2
 \end{aligned} \tag{11}$$

Variance of a linear function of X

$$\begin{aligned}
 \text{Var}[a + bX] &= b^2 \mathbb{E}[(X - \mu_x)^2] \\
 &= b^2 \text{Var}[X]
 \end{aligned} \tag{12}$$

Variance of a linear function of two random variables X and Y

$$\text{Var}[a + bX + cY] = b^2 \text{Var}[X] + c^2 \text{Var}[Y] + 2bc \text{cov}[X, Y] \tag{13}$$

Variance of a linear function of uncorrelated random variables

$$\text{Var}[a_0 + a_1 X_1 + a_2 X_2 + \dots + a_n X_n] = a_1^2 \text{Var}[X_1] + a_2^2 \text{Var}[X_2] + \dots + a_n^2 \text{Var}[X_n] \tag{14}$$

2.5 Covariance and Correlation

Covariance

$$\begin{aligned}
 \text{cov}[X, Y] &= \mathbb{E}[(X - \mu_x)(Y - \mu_y)] \\
 &= \mathbb{E}[XY] - \mathbb{E}[X]\mathbb{E}[Y]
 \end{aligned} \tag{15}$$

$$\begin{aligned}
\text{cov}[X, X] &= \text{E}[(X - \mu_x)^2] \\
&= \text{E}[X^2] - (\text{E}[X])^2 \\
&= \text{Var}[X] \\
&= \sigma_x^2
\end{aligned} \tag{16}$$

Correlation Coefficient

$$\begin{aligned}
\rho &= \frac{\text{cov}[X, Y]}{\sigma_x \sigma_y} \\
-1 &\leq \rho \leq 1
\end{aligned} \tag{17}$$

3. The first order second moment (FOSM) method

The First Order Second Moment (FOSM) method is a relatively simple method of including the effects of variability of input variables on a resulting dependent variable

The First Order Second Moment method uses a Taylor series expansion of the function to be evaluated. This expansion is truncated after the linear term, (hence “first order”). The modified expansion is then used, along with the first two moments of the random variable(s), to determine the values of the first two moments of the dependent variable (hence “second moment”).

Due to truncation of the Taylor series after first order terms, the accuracy of the method deteriorates if second and higher derivatives of the function are significant. Furthermore, the method takes no account of the form of the probability density function, describing the random variables using only their mean and standard deviation. The skewness (third moment) and higher moments are ignored.

Another limitation of the traditional FOSM method is that explicit account of spatial correlation of the random variable is not typically done. For example, the soil properties at two geotechnical sites could have identical mean and standard deviations, however at one site, the properties could vary rapidly from point to point (“low” spatial correlation length), and at another they could vary gradually (“high spatial correlation length”). This issue will be returned to later in the paper.

Consider a function $f(X, Y)$ of two random variables X and Y .

The Taylor Series expansion of the function about the mean values (μ_x, μ_y) , truncated after first order terms from equation (8), gives:

$$f(X, Y) \approx f(\mu_x, \mu_y) + (X - \mu_x) \frac{\partial f}{\partial x} + (Y - \mu_y) \frac{\partial f}{\partial y} \tag{18}$$

where derivatives are evaluated at (μ_x, μ_y) .

To a first order of accuracy, the expected value of the function is given by equation (9), and the variance by,

$$\text{Var}[f(X, Y)] \approx \text{Var}[(X - \mu_x) \frac{\partial f}{\partial x} + (Y - \mu_y) \frac{\partial f}{\partial y}] \tag{19}$$

hence,

$$\text{Var}[f(X, Y)] \approx \left(\frac{\partial f}{\partial x}\right)^2 \text{Var}[X] + \left(\frac{\partial f}{\partial y}\right)^2 \text{Var}[Y] + 2 \frac{\partial f}{\partial x} \frac{\partial f}{\partial y} \text{cov}[X, Y] \tag{20}$$

If X and Y are uncorrelated,

$$\text{Var}[f(X, Y)] \approx \left(\frac{\partial f}{\partial x}\right)^2 \text{Var}[X] + \left(\frac{\partial f}{\partial y}\right)^2 \text{Var}[Y] \quad (21)$$

In general, for a function of n uncorrelated random variables, the FOSM Method gives:

$$\text{Var}[f(X_1, X_2, \dots, X_n)] \approx \sum_{i=1}^n \left(\frac{\partial f}{\partial x_i}\right)^2 \text{Var}[X_i] \quad (22)$$

where the first derivatives are evaluated at the mean values $(\mu_{x_1}, \mu_{x_2}, \dots, \mu_{x_n})$

3.1 FOSM Example: Passive earth pressure against a smooth wall

The limiting horizontal passive earth force against a smooth wall of height H is given from the Rankine equation as:

$$P_p = \frac{1}{2}\gamma H^2 K_p + 2c' H \sqrt{K_p} \quad (23)$$

where the passive earth pressure coefficient is written in this case as:

$$K_p = [\tan \phi' + (1 + \tan^2 \phi')^{1/2}]^2 \quad (24)$$

in order to emphasize the influence of the fundamental variable $\tan \phi'$.

In dimensionless form we can write:

$$\frac{P_p}{\gamma H^2} = \frac{1}{2}K_p + 2\sqrt{K_p} \frac{c'}{\gamma H} \quad (25)$$

or

$$\bar{P}_p = \frac{1}{2}K_p + 2\bar{c}\sqrt{K_p} \quad (26)$$

where \bar{P}_p is a dimensionless passive earth force, and \bar{c} is a dimensionless cohesion.

Operating on equation (26) and treating $\tan \phi'$ and \bar{c} as uncorrelated random variables, from equation (9),

$$\mu_{\bar{P}_p} = \text{E}[\bar{P}_p] = \frac{1}{2}\mu_{K_p} + 2\mu_{\bar{c}}\sqrt{\mu_{K_p}} \quad (27)$$

and from equation (22),

$$\sigma_{\bar{P}_p}^2 = \text{Var}[\bar{P}_p] = \left(\frac{\partial \bar{P}_p}{\partial \bar{c}}\right)^2 \text{Var}[\bar{c}] + \left(\frac{\partial \bar{P}_p}{\partial (\tan \phi')}\right)^2 \text{Var}[\tan \phi'] \quad (28)$$

The required derivatives computed analytically from equation (26) are given by:

$$\frac{\partial \bar{P}_p}{\partial \bar{c}} = 2\sqrt{\mu_{K_p}} \quad (29)$$

and

$$\frac{\partial \bar{P}_p}{\partial(\tan \phi')} = \frac{\mu_{K_p}}{\sqrt{1 + \mu_{\tan \phi'}^2}} + 2\mu_{\bar{c}} \frac{\sqrt{\mu_{K_p}}}{\sqrt{1 + \mu_{\tan \phi'}^2}} \quad (30)$$

where the derivatives are evaluated at the means.

It is now possible to compute the mean and standard deviation of the horizontal earth force for a range of input soil property variances. In this example, the Coefficient of Variation (V) values for both \bar{c} and $\tan \phi'$ are the same, thus

$$V_{\bar{c}, \tan \phi'} = \frac{\sigma_{\bar{c}}}{\mu_{\bar{c}}} = \frac{\sigma_{\tan \phi'}}{\mu_{\tan \phi'}} \quad (31)$$

Table 1, shows the influence of variable input on the passive force in the case of $\mu_{\bar{c}} = 5$ and $\mu_{\tan \phi'} = \tan 30^\circ = 0.577$. It can be seen that in this case the process results in a slight magnification of the Coefficient of Variation of the passive force over the input values. For example, $V_{\bar{c}, \tan \phi'} = 0.5$ leads to $V_{\bar{P}_p} = 0.53$ and so on.

Table 1. Statistics of \bar{P}_p predicted using FOSM (analytical approach)
 $\mu_{\bar{c}} = 5$ and $\mu_{\tan \phi'} = \tan 30^\circ = 0.577$

$V_{\bar{c}, \tan \phi'}$	$\partial \bar{P}_p / \partial \bar{c}$	$\text{Var}[\bar{c}]$	$\partial \bar{P}_p / \partial(\tan \phi')$	$\text{Var}[\tan \phi']$	$\text{Var}[\bar{P}_p]$	$\sigma_{\bar{P}_p}$	$\mu_{\bar{P}_p}$	$V_{\bar{P}_p}$
0.1	3.46	0.25	17.60	0.0033	4.03	2.01	18.82	0.11
0.3	3.46	2.25	17.60	0.0300	36.29	6.02	18.82	0.32
0.5	3.46	6.25	17.60	0.0833	100.81	10.04	18.82	0.53
0.7	3.46	12.25	17.60	0.1633	197.59	14.06	18.82	0.75
0.9	3.46	20.25	17.60	0.2700	326.64	18.07	18.82	0.96

The ratio of the output $V_{\bar{P}_p}$ to the input $V_{\bar{c}, \tan \phi'}$ can also be obtained analytically from equations (27) and (28) to give:

$$\frac{V_{\bar{P}_p}}{V_{\bar{c}, \tan \phi'}} \approx 2 \frac{\sqrt{(\sqrt{\mu_{K_p}} + 2\mu_{\bar{c}})^2 (\mu_{K_p} - 1)^2 + 4\mu_{\bar{c}}^2 (\mu_{K_p} + 1)^2}}{(\sqrt{\mu_{K_p}} + 4\mu_{\bar{c}})(\mu_{K_p} + 1)} \quad (32)$$

This equation is plotted in Figure 1 for a range of $\mu_{\bar{c}}$ values. The graph indicates that in many cases, the FOSM method causes the ratio given by equation (32) to be less than unity. In other words the Coefficient of Variation of the output passive force is smaller than the Coefficient of Variation of the input strength parameters. For higher friction angles however this trend is reversed.

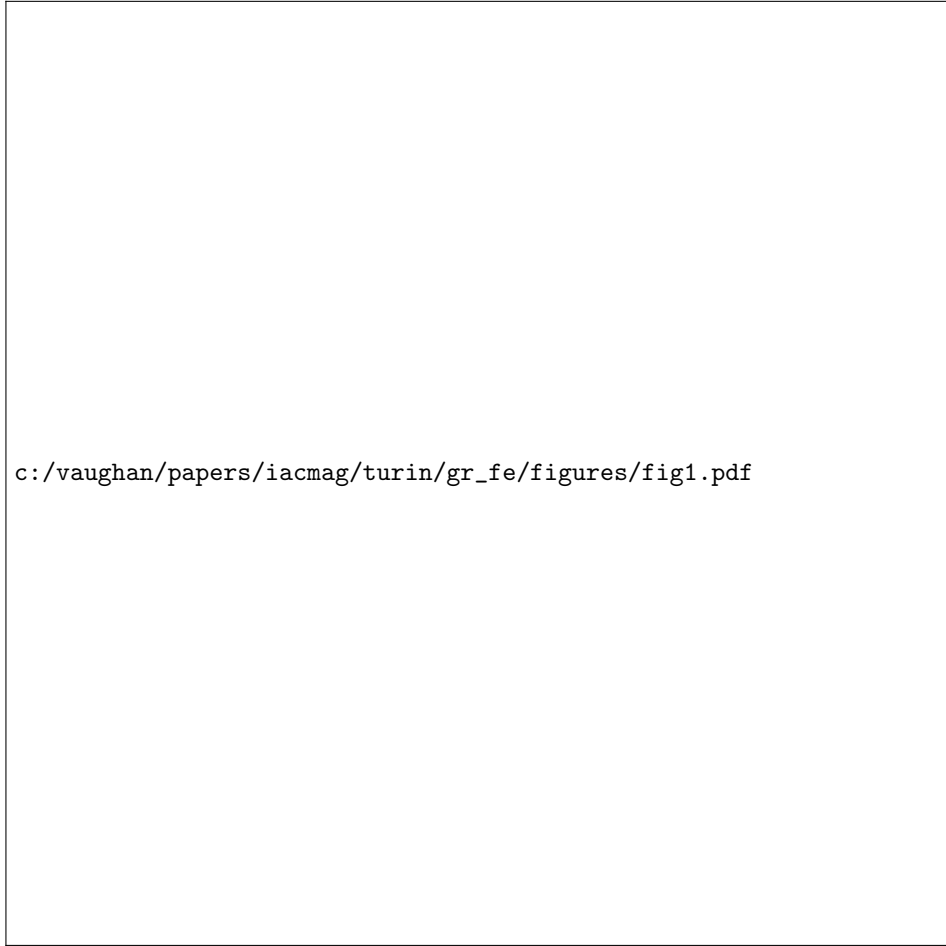


Figure 1. $\frac{V_{\bar{P}_p}}{V_{\bar{c}, \tan \phi'}}$ vs. $\mu_{\tan \phi'}$ for passive earth pressure analysis by FOSM

3.1.1 Numerical approach

An alternative approach evaluates the derivatives numerically, using a central finite difference formula. In this case, the dependent variable, \bar{P}_p , is sampled across two standard deviations in one variable, while keeping the other variable fixed at the mean. This large central difference interval encompasses about 68% of all values of the input parameters \bar{c} and $\tan \phi'$, so the approximation is only reasonable if the function \bar{P}_p from equation (26), does not exhibit much nonlinearity across this range. The finite difference formulas take the form:

$$\frac{\partial \bar{P}_p}{\partial \bar{c}} \approx \frac{\bar{P}_p(\mu_{\bar{c}} + \sigma_{\bar{c}}, \mu_{\tan \phi'}) - \bar{P}_p(\mu_{\bar{c}} - \sigma_{\bar{c}}, \mu_{\tan \phi'})}{2\sigma_{\bar{c}}} = \frac{\Delta P_{p(\bar{c})}}{2\sigma_{\bar{c}}} \quad (33)$$

and

$$\frac{\partial \bar{P}_p}{\partial (\tan \phi')} \approx \frac{\bar{P}_p(\mu_{\bar{c}}, \mu_{\tan \phi'} + \sigma_{\tan \phi'}) - \bar{P}_p(\mu_{\bar{c}}, \mu_{\tan \phi'} - \sigma_{\tan \phi'})}{2\sigma_{\tan \phi'}} = \frac{\Delta P_{p(\tan \phi')}}{2\sigma_{\tan \phi'}} \quad (34)$$

The main attraction of this approach, is that once the derivative terms are squared and substituted into equation (28), the variances of \bar{c} and $\tan \phi'$ cancel out, leaving:

$$\text{Var}[\bar{P}_p] \approx \left(\frac{\Delta \bar{P}_{p(\bar{c})}}{2} \right)^2 + \left(\frac{\Delta \bar{P}_{p(\tan \phi')}}{2} \right)^2 \quad (35)$$

In this case, \bar{P}_p is a linear function of \bar{c} and is slightly nonlinear with respect to $\tan \phi'$. It is clear from a comparison of Tables 1 and 2, that the numerical and analytical approaches in this case give essentially the same results.

Table 2. Statistics of \bar{P}_p predicted using FOSM (numerical approach)
 $\mu_{\bar{c}} = 5$ and $\mu_{\tan \phi'} = \tan 30^\circ = 0.577$

$V_{\bar{c}, \tan \phi'}$	$\frac{\Delta \bar{P}_{p(\bar{c})}}{2}$	$\frac{\Delta \bar{P}_{p(\tan \phi')}}{2}$	$\text{Var}[\bar{P}_p]$	$\sigma_{\bar{P}_p}$	μ_{q_u}	$V_{\bar{P}_p}$
0.1	1.73	1.02	4.03	2.01	18.82	0.11
0.3	5.20	3.04	36.26	6.02	18.82	0.32
0.5	8.66	5.05	100.53	10.03	18.82	0.53
0.7	12.12	7.04	196.54	14.02	18.82	0.74
0.9	15.59	9.00	323.93	18.00	18.82	0.96

3.1.2 Refined approach including second order terms

In the above example, a first order approximation was used to predict both the mean and variance of \bar{P}_p from equations (9) and (19). Since the variances of \bar{c} and $\tan \phi'$ are both known, it is possible to refine the estimate of $\mu_{\bar{P}_p}$ by including second order terms from equation (10) leading to:

$$\begin{aligned} \mu_{\bar{P}_p} \approx & \bar{P}_p(\mu_{\bar{c}}, \mu_{\tan \phi'}) + \frac{1}{2} \text{Var}[\bar{c}] \frac{\partial^2 \bar{P}_p}{\partial \bar{c}^2} + \frac{1}{2} \text{Var}[\tan \phi'] \frac{\partial^2 \bar{P}_p}{\partial (\tan \phi')^2} \\ & + \text{cov}[\bar{c}, \tan \phi'] \frac{\partial^2 \bar{P}_p}{\partial \bar{c} \partial (\tan \phi')} \end{aligned} \quad (36)$$

where all derivatives are evaluated at the mean. Noting that in this case $\partial^2 \bar{P}_p / \partial \bar{c}^2 = 0$, and $\text{cov}[\bar{c}, \tan \phi'] = 0$, the expression simplifies to:

$$\mu_{\bar{P}_p} \approx \bar{P}_p(\mu_{\bar{c}}, \mu_{\tan \phi'}) + \frac{1}{2} \text{Var}[\tan \phi'] \frac{\partial^2 \bar{P}_p}{\partial (\tan \phi')^2} \quad (37)$$

where the analytical form of the second derivative is given by:

$$\frac{\partial^2 \bar{P}_p}{\partial (\tan \phi')^2} = \frac{2}{1 + \mu_{\tan \phi'}^2} [\mu_{K_p} + \mu_{\bar{c}} \sqrt{\mu_{K_p}}] - \frac{\mu_{\tan \phi'}}{(1 + \mu_{\tan \phi'}^2)^{3/2}} [\mu_{K_p} + 2\mu_{\bar{c}} \sqrt{\mu_{K_p}}] \quad (38)$$

Combining equations (37) and (38) for the particular case of $\mu_{\bar{c}} = 5$ and $\mu_{\tan \phi'} = 0.577$ leads to:

$$\mu_{\bar{P}_p} = 18.82 + 4.94 \text{ Var}[\tan \phi'] \quad (39)$$

Table 3 shows a reworking of the analytical results from Table 1 including second order terms in the estimation of $\mu_{\bar{P}_p}$. A comparison of the results from the two tables indicates that the second order terms have marginally increased $\mu_{\bar{P}_p}$ and thus reduced $V_{\bar{P}_p}$. The differences introduced by the second order terms are quite modest however, indicating the essentially linear nature of this problem.

Table 3. Statistics of \bar{P}_p predicted using FOSM
(analytical approach including second order terms)
 $\mu_{\bar{c}} = 5$ and $\mu_{\tan \phi'} = \tan 30^\circ = 0.577$

$V_{\bar{c}, \tan \phi'}$	$\text{Var}[\tan \phi']$	$\sigma_{\bar{P}_p}$	$\mu_{\bar{P}_p}$	$V_{\bar{P}_p}$
0.1	0.0033	2.01	18.84	0.11
0.3	0.0300	6.02	18.97	0.32
0.5	0.1833	10.04	19.23	0.52
0.7	0.1633	14.06	19.63	0.72
0.9	0.2700	18.07	20.15	0.90

4 The Hasofer-Lind method (FORM)

The major drawback to the FOSM method, as pointed out by Ditlevson (1973), is that it can give different failure probabilities for the same problem when stated in equivalent, but different, ways. See also Madsen *et al* (1986) and Baecher and Christian (2003) for detailed comparisons of these methods. A short discussion of the non-uniqueness of FOSM is worth giving here, since it is this non-uniqueness that motivated Hasofer and Lind (1974) to develop an improved approach.

A key quantity of interest following an analysis using FOSM or FORM is the determination of the reliability index, β , for a given safety margin, M . The reliability index, β , as defined by Cornell (1969) is

$$\beta = \frac{\text{E}[M]}{\sqrt{\text{Var}[M]}} \quad (40)$$

which measures how far the mean of the safety margin is from zero (assumed to be the failure point) in units of number of standard deviations. In the classical resistance (R) versus load (L) problem, the safety margin (M) can be defined as

$$M = R - L \quad (41)$$

so that failure occurs if $M < 0$ and interest focuses on the probability of this event happening. Since owners and politicians do not like to hear about probabilities of failure, this probability is codified using the rather more obscure reliability index. There is however a unique relationship between the reliability index (β) and the probability of failure (p_f) given by:

$$p_f = 1 - \Phi(\beta) \quad (42)$$

assuming that R and L are normally distributed independent random variables, where $\Phi(\beta)$ is the area under a standard normal distribution curve to the left of β as given by standard tables. In the context of passive earth pressure analysis, L might be the load applied to an anchor block, and R might be the limiting passive resistance available.

The line, or surface in higher dimensions, defined by $M = 0$ is called the *failure surface*.

If R is independent of L , then the FOSM method gives from equations (9) and (22):

$$\text{E}[M] \simeq \text{E}[R] - \text{E}[L] = \mu_R - \mu_L$$

and

$$\text{Var} [M] \simeq \left(\frac{\partial M}{\partial R} \right)^2 \text{Var} [R] + \left(\frac{\partial M}{\partial L} \right)^2 \text{Var} [L] = \text{Var} [R] + \text{Var} [L] = \sigma_R^2 + \sigma_L^2 \quad (43)$$

(note that because the safety margin is linear in this case, the first-order mean and variance of M are exact) so that

$$\beta = \frac{\mu_R - \mu_L}{\sqrt{\sigma_R^2 + \sigma_L^2}} \quad (44)$$

For non-negative resistance and loads, as is typically the case in Civil engineering, the safety margin can equivalently be defined as

$$M = \ln \left(\frac{R}{L} \right) = \ln(R) - \ln(L) \quad (45)$$

so that failure occurs if $M < 0$, as before. In this case,

$$\text{E} [M] \simeq \ln(\mu_R) - \ln(\mu_L) \quad (46)$$

which is clearly no longer the same as before, and

$$\begin{aligned} \text{Var} [M] &\simeq \left(\frac{\partial M}{\partial R} \right)^2 \text{Var} [R] + \left(\frac{\partial M}{\partial L} \right)^2 \text{Var} [L] \\ &= \frac{\text{Var} [R]}{R^2} + \frac{\text{Var} [L]}{L^2} \quad (\text{to be evaluated at the means}) \\ &= V_R^2 + V_L^2 \end{aligned} \quad (47)$$

where V_R and V_L are the coefficients of variation of R and L respectively. This gives a different reliability index,

$$\beta = \frac{\ln(\mu_R) - \ln(\mu_L)}{\sqrt{V_R^2 + V_L^2}} \quad (48)$$

The non-uniqueness of the FOSM method is due to the fact that different functional representations may have different mean estimates and different first derivatives. What the FOSM method is doing is computing the distance from the mean point to the failure surface *in the direction of the gradient at the mean point*. Hasofer and Lind (1974) solved the non-uniqueness problem by looking for the minimum distance between the mean point and the failure surface, rather than looking just along the gradient direction.

In the general case, suppose that the safety margin, M , is a function of a sequence of random variables, $\mathbf{X} = \{X_1, X_2, \dots\}$,

$$M = f(X_1, X_2, \dots) \quad (49)$$

and that the random variables X_1, X_2, \dots have covariance matrix $\underline{\underline{C}}$. Then the Hasofer-Lind reliability index is defined by

$$\beta = \min_{M=0} \sqrt{(x - E[X])^T \underline{\underline{C}}^{-1} (x - E[X])} \quad (50)$$

which is the minimum distance between the failure surface ($M = 0$) and the mean point ($E[X]$) in units of number of standard deviations ($\underline{\underline{C}}^{-1}$). Finding β under this definition is iterative; choose a value of x_0 which lies on the curve $M = 0$ and compute a guess at β_0 , choose another point x_1 on $M = 0$ and compute another β_1 , and so on. The Hasofer-Lind reliability index is the minimum of all such possible values of β_i .

In practice, there are a number of sophisticated optimization algorithms, generally involving the gradient of M , which find the point where the failure surface is perpendicular to the line to the origin. The distance between these two points is β . Many spreadsheet programs now include such algorithms, and the user need only specify the minimization equation (see above) and the constraints on the solution (ie. that x is selected from the curve $M = 0$ in this case). Unfortunately, many non-linear failure surfaces have multiple local minima, with respect to the mean point, which further complicates the problem. In this case, techniques such as Simulated Annealing (see Numerical Recipes, 1997) may be necessary, but which do not guarantee finding the global minimum. Monte Carlo simulation, to be considered next, is an approach which is simple in concept and which can be extended easily to very difficult failure problems with only a penalty in computing time to achieve a high level of accuracy.

5 Random field/finite element approach (RFEM)

For reasonably “linear” problems, the FOSM and FORM methods described in this paper are able to take account of soil property variability in a systematic way. The traditional methods however, typically take no account of spatial correlation, which is the tendency for properties of soil elements “close together” to be correlated, while soil elements “far apart” are uncorrelated. In soil failure problems such as passive earth pressure analysis, it is possible to account for local averaging and spatial correlation by prescribing a potential failure surface and averaging the soil strength parameters along it (e.g. Peschl and Schweiger 2003). A disadvantage of this approach is that the location of the potential failure surface must be anticipated in advance, which rather defeats the purpose of a general random soil model.

To address the correlation issue, the passive earth pressure problem has been reanalyzed using the random finite element method (RFEM), enabling soil property variability and spatial correlation to be accounted for in a rigorous and general way. The methodology involves the generation and mapping of a random field of c' and $\tan \phi'$ properties onto a quite refined finite element mesh. Full account is taken of local averaging and variance reduction (Fenton and Vanmarcke 1990) over each element, and an exponentially decaying spatial correlation function is incorporated. An elasto-plastic finite element analysis is then performed using a Mohr-Coulomb failure criterion (see e.g. Griffiths and Fenton (2001) for further details).

In a passive earth pressure analysis the nodes representing the rigid wall are translated horizontally into the mesh and the reaction forces back-figured from the developed stresses. The limiting passive resistance (P_p) is eventually reached and the analysis is repeated numerous times using Monte-Carlo simulations. Each realization of the Monte-Carlo process involves

a random field with the same mean, standard deviation and spatial correlation length. The spatial distribution of properties varies from one realization to the next however, so that each simulation leads to a different value of P_p . The analysis has the option of including cross correlation between properties and anisotropic spatial correlation lengths (e.g. the spatial correlation length in a naturally occurring stratum of soil is often higher in the horizontal direction). Neither of these options has been investigated in the current study to facilitate comparisons with the simpler methods.

Lognormal distributions of c' and $\tan \phi'$ have been used in the current study and mapped onto a mesh of 8-node, quadrilateral, plane strain elements. Examples of different spatial correlation lengths are shown in Figure 2 in the form of a grey scale in which weaker regions are darker, and stronger regions are lighter.

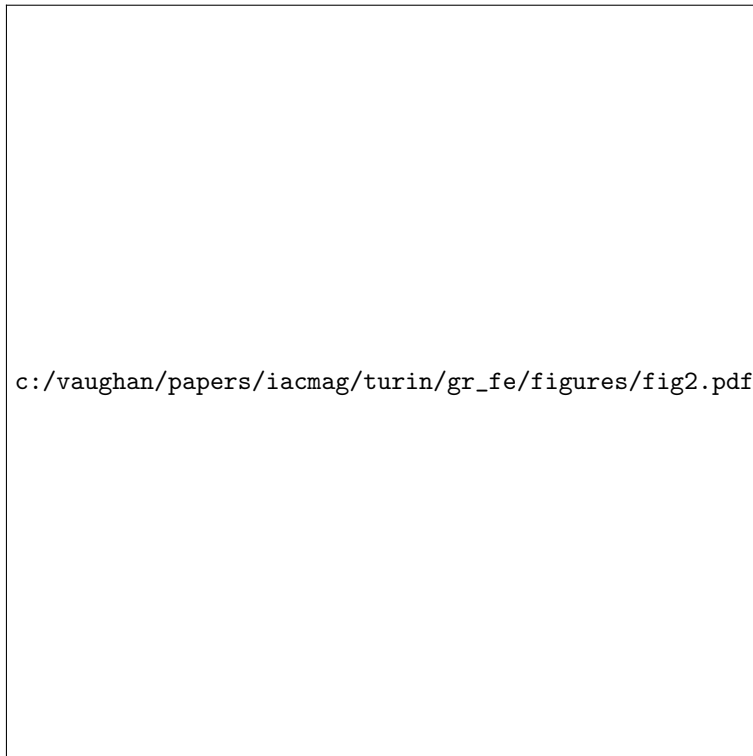


Figure 2. Typical random fields in the RFEM approach

An example of a relatively low spatial correlation length and a relatively high correlation length are shown. It should be emphasized that the mean and standard deviation of the random variable being portrayed are the same in both figures. The spatial correlation length (which has units of length) is defined with respect to the underlying normal distribution, and denoted as $\theta_{\ln c', \ln \tan \phi'}$. Both c' and $\tan \phi'$ were assigned the same isotropic correlation length in this study. A convenient non-dimensional form of the spatial correlation length can be achieved in the earth pressure analysis by dividing by the wall height H , thus $\Theta = \theta_{\ln c', \ln \tan \phi'} / H$.

5.1 Parametric studies

A quite extensive set of parametric studies of the passive earth pressure problem by RFEM were performed by Tveten(2002). A few of these results are presented here in which the Coefficients of Variation of c' and $\tan \phi'$, and spatial correlation length Θ have been varied. In all cases, the mean strength parameters have been held constant at $\mu_{c'} = 100$ kPa and $\mu_{\tan \phi'} = \tan 30^\circ = 0.577$. In addition, the soil unit weight was fixed at 20kN/m^3 , and the wall height set to unity. Thus, the dimensionless cohesion described earlier in the paper is given by $\bar{c} = c' / (\gamma H) = 5$. The variation in the limiting mean passive earth pressure, μ_{P_p} , normalized with respect to the value that would be given by simply substituting the mean strength values $P_p(\mu_{c'}, \mu_{\tan \phi'}) = 376.4$ kN/m, is shown in Figures 3.

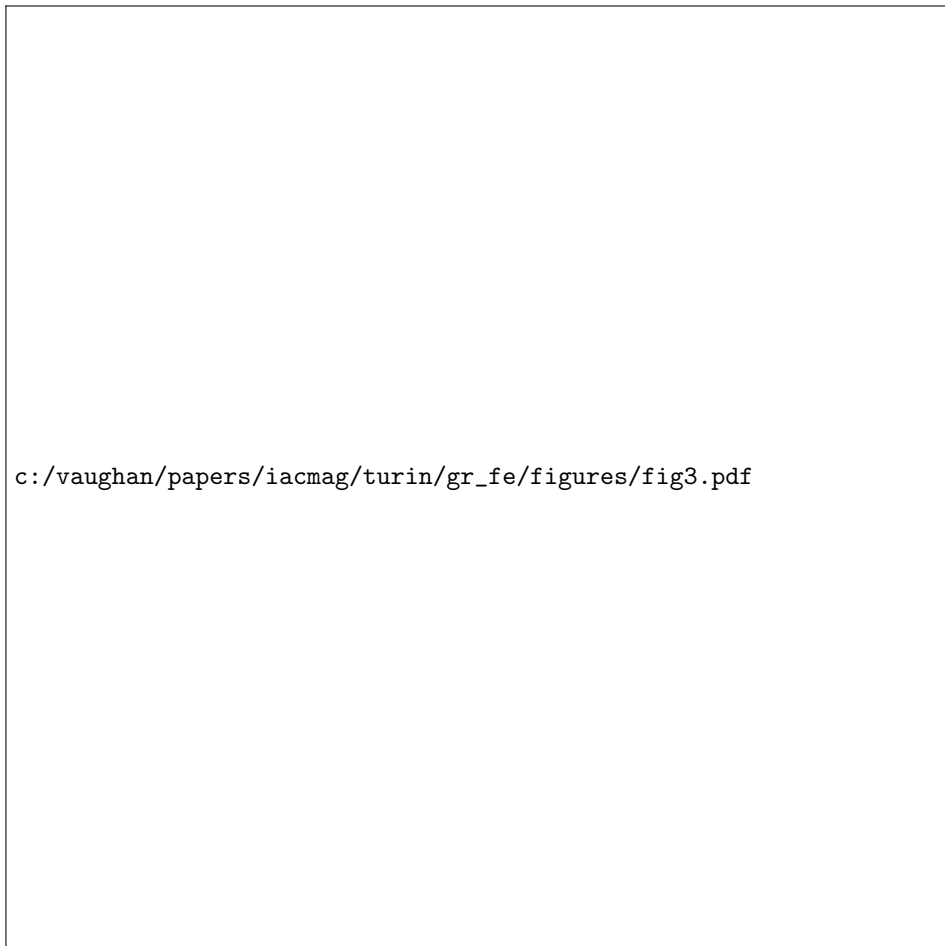


Figure 3. Influence of Θ on normalized μ_{P_p} for different $V_{\bar{c}, \tan \phi'}$

The figure shows results for spatial correlation lengths in the range $0.01 < \Theta < 10$. At the lower end, the small spatial correlation lengths result in very significant local averaging over each finite element. In the limit as $\Theta \rightarrow 0$, local averaging causes the mean of the properties to tend to the Median and the variance to tend to zero (see e.g. Griffiths and Fenton 2004). For a typical random variable X , the properties of the lognormal distribution give that:

$$\frac{\text{Median}_X}{\mu_X} = \frac{1}{(1 + V_X)^{1/2}} \quad (51)$$

With reference to Figure 3 and the curve corresponding to $V_{\bar{c}, \tan \phi'} = 0.8$, the ratio given by equation (51) is 0.781. For a soil with $\mu_{c'} = 100$ kPa and $\mu_{\tan \phi'} = \tan 30^\circ = 0.577$, as $\Theta \rightarrow 0$, these properties tend to $\text{Median}_{c'} = 78.1$ kPa and $\text{Median}_{\tan \phi'} = 0.451$ respectively. The limiting passive earth pressure with these Median values is 265.7 kN/m, which leads to a normalized value of 0.71 as indicated at the left side of Figure 3

At the other extreme, as $\Theta \rightarrow \infty$, there is no local averaging and each realization of the Monte-Carlo leads to an analysis of a uniform soil. In this case there is no reduction of strength due to local averaging and the lines in Figure 3 all tend to unity on the right side. This is essentially the result indicated by the FOSM analysis.

All the lines indicate a slight minimum in the limiting passive resistance occurring close to, or slightly lower than, $\Theta \approx 1$. This value of Θ implies a spatial correlation length of the order of the height of the wall itself. Similar behavior was observed by Griffiths and Fenton (2001) in relation to bearing capacity analysis. It is speculated that at this spatial correlation length, there is a greater likelihood of weaker zones of soil aligning with each other facilitating the formation of a failure mechanism.

The above discussion highlights the essential difference and benefits offered by the RFEM method over conventional probabilistic. These can be summarized as follows:

- The RFEM accounts for spatial correlation in a rigorous and objective way.
- The RFEM does not require the user to anticipate the location or length of the failure mechanism. The mechanism forms naturally wherever the surface of least resistance happens to be.

Figure 4. Typical passive failure mechanism. Dark zones indicate weaker soil.

Figure 4 shows the deformed mesh at failure from a typical realization of the Monte-Carlo process. It can be seen that in this case the weaker dark zone near the ground surface has triggered a quite localized mechanism that outcrops at this location.

Some other differences between FOSM and RFEM worth noting are as follows:

- 1) Figure 3 indicates that for intermediate values of Θ , the RFEM results show a fall and even a minimum in the μ_{P_p} as $V_{c', \tan \phi'}$ response as Θ is reduced, while FOSM gave essentially constant values. In fact, when second order terms were included (Table 3) a slight *increase* in μ_{P_p} was observed.
- 2) Tables 1-3 using FOSM indicated that the Coefficient of Variation of the passive earth force was similar to the Coefficient of Variation of the input shear strength parameters. Due to local averaging in the RFEM on the other hand, the Coefficient of Variation of the passive earth force falls as Θ is reduced. As $\Theta \rightarrow 0$ in the RFEM approach, the Coefficient of Variation of the passive force also tends to zero.

6 Discussion and concluding remarks

The paper has discussed three methods for implementing probabilistic concepts into geotechnical analysis of a simple problem of passive earth pressure. The “simple” methods were the



c:/vaughan/papers/iacmag/turin/gr_fe/figures/fig4.pdf

First Order Second Moment (FOSM) and First Order Reliability Method (FORM), and the “sophisticated” method was the Random Finite Element Method method (RFEM).

1) Probabilistic methods offer a more rational way of approaching geotechnical analysis, in which probabilities of design failure can be assessed. This is more meaningful than the abstract “Factor of Safety” approach. Being relatively new however, probabilistic concepts can be quite difficult to digest, even in the so called “simple” methods.

2) The RFEM method indicates a significant reduction in mean compressive strength due to the weaker zones dominating the overall strength at intermediate values of Θ . The observed reduction in the mean strength by RFEM, is greater than could be explained by local averaging alone.

3) The paper has shown that proper inclusion of spatial correlation, as used in the RFEM, is essential for quantitative predictions in probabilistic geotechnical analysis. While “simpler” methods such as FOSM and FORM are useful for giving guidance on the sensitivity of design outcomes to variations of input parameters, their inability to systematically include spatial correlation and local averaging limits their usefulness.

4) The paper has shown that the RFEM is one of the very few methods available for modeling highly variable soils in a systematic way. In the analysis of soil masses, such as the passive earth pressure problem considered herein, a crucial advantage of RFEM is that it allows the failure mechanism to “seek out” the critical path through the soil.

References

Acknowledgement

The writers acknowledge the support of NSF Grant No. CMS-0408150.